Excitons in self-organized semiconductor/insulator superlattices: PbI-based perovskite compounds

E. A. Muljarov, S. G. Tikhodeev,* and N. A. Gippius
General Physics Institute, Russian Academy of Sciences, Vavilova Street 38, Moscow 117333, Russia

Teruya Ishihara†
Department of Physical Electronics, Faculty of Engineering, Hiroshima University, Kagamiyama, Higashi-Hiroshima 724, Japan
(Received 14 November 1994)

We calculate the binding energies, wave functions, and diamagnetic coefficients of excitons in perovskite lead iodide based compounds in the form of self-organized semiconductor/insulator superlattices with allowance for the image potential and the superlattice structure of these materials. We demonstrate a good agreement between our theory and the experiment; the fitting of our theory to the experiments makes it possible to evaluate the reduced mass of excitons in these compounds of the order of $0.2m_0$.

I. INTRODUCTION

Recently there has been considerable progress in the growth of a large class of self-organized perovskite lead iodide based compounds with pronounced excitonic properties.[1–7] These compounds may be regarded as semiconductor/insulator (S/I) multiple-quantum-well (MQW) structures[2] consisting of lead iodide semiconductor layers sandwiched between alkylammonium (or phenethylammonium) insulator layers, with energy gap more than three times larger than that of the PbI layers. These materials are of great interest because of possible optoelectronic applications due to the pronounced excitonic effects.

The lead iodide compounds have a chemical formula $(RNH_3)_2(CH_3NH_3)_{m-1}Pb_mI_{3m+1}$, where R stands for either a hydrocarbon chain C_nH_{2n+1} or a phenethyl group $C_6H_5C_2H_4$. The former corresponds to the alkylammonium family $(C_nH_{2n+1}NH_3)_2PbI_4$, abbreviated as C_n-PbI_4 (here $m = 1$), with n integer. The latter corresponds to the phenethylammonium family $(C_6H_5C_2H_4NH_3)_2(CH_3NH_3)_{m-1}Pb_mI_{3m+1}$, abbreviated as PhE-$Pb_mI_{3m+1}$, with $m = 1, 2$. The thickness of insulator (organic) layers increases with increase of n in the C_n-PbI_4 family, and the semiconductor (lead iodide) layer thickness in PhE-Pb_2I_7 is twice as large as in the PbI_4 family. Also the dielectric constant of the insulator layers in the PhE family (about 2.34) is larger than in the C_n-PbI_4 one (about 2.1). The ultimate member $CH_3NH_3PbI_3$ ($m = \infty$), or C_1-PbI_3, according to our abbreviation, is also known.[6] This structure lacks insulator layers and can be considered as a three-dimensional (3D) version. As a result, lead iodide self-organized compounds represent an interesting example of S/I superlattices (SL's) with different ratios of barrier to well thicknesses and dielectric constants.

Excitons in PbI-based S/I MQW compounds are significantly enhanced as compared to the 3D version. The exciton binding energy varies from 170 to 330 meV in C_n-PbI_4 and PhE-PbI families,[3] while it is only 45 meV in C_1-PbI_3.[6]

The enhancement of an exciton in quasi-2D systems is a well-known phenomenon—for example, the spatial electron and hole confinement in a very thin and deep QW quadruples the exciton binding energy and halves the exciton Bohr radius. This is not the case of the PbI-based compounds where the exciton radius is comparable with the layer width; 2D potential confinement is still effective, but not enough to explain the enhancement. It was shown in Refs. 2, 3, and 5 that the exciton enhancement in PbI-based compounds may be attributed to alternating semiconductor and insulator layers with considerably different dielectric constants (about 6 and 2, respectively), causing an image-potential-magnified electron-hole (e-h) attraction.

This effect of the so-called dielectric confinement of excitons was predicted by Rytova[8] and Keldysh,[9] who investigated excitons in a thin semiconductor film in dielectric surroundings. The variational approach to the same problem in a single quantum well was developed by Hanamura *et al.*[10] (see also Ref. 11 for quantum dots). In III-V semiconductor/semiconductor nanostructures such as $GaAs/Al_xGa_{1-x}As$, the difference between dielectric constants of adjoining layers is not large (usually of the order of 10 %), and the effect of the dielectric confinement of excitons is small.[12] However, in II-VI nanostructures and especially in III-V/II-VI ones (see, e.g., Ref. 13) the difference between the dielectric constants of adjacent layers and thus the dielectric confinement of excitons may be comparatively large. And in semiconductor/insulator nanostructures, such as lead iodide based self-organized SL's, the effect of dielectric confinement should be exceptionally significant.

The variational approach of Ref. 10 was used in Refs. 2 and 5 for theoretical investigation of excitons in PbI-based compounds. However, within this approach the interaction of QW-localized electrons and holes with their

own images (self-image terms) is not taken into account correctly. Moreover, the calculations in Refs. 2 and 5 were made for a single QW, without taking the SL effects into account.

The purpose of the present paper is to calculate the exciton wave functions, binding energies, radii, and diamagnetic factors in semiconductor/insulator superlattices with special emphasize on the PbI-based perovskite compounds. We use a standard approach for the theory of heterostructures treating different lead iodide based compounds as MQW structures, postulating the parameters of "parent" well and barrier materials for each lead iodide family, and changing only the layers' thickness. Our model demonstrates a good agreement with the experimental data on excitons in lead iodide based compounds, if we take into account the image potentials (including the self-image corrections) and the superlattice (SL) effects.

The SL effects lead to the dependence of exciton parameters on the insulator layer width in the C_n-PbI_4 family. In the present paper, we consider the SL effects on the image potentials only (following the approach of Guseinov[14]), but we neglect the overlap of the electron and hole wave functions between different QW's. The barrier heights and widths of insulator layers in all PbI-based compounds are large enough to make the tunneling between neighboring layers negligibly small. In other words, we treat the PbI-based compounds as MQW structures, neglecting the width of the SL minibands. As to the self-image terms, we include them into the one-electron and the one-hole QW-localizing potential, contrary to the approach of Ref. 15. The self-image interaction does not depend on the in-plane e-h distance, and modifies basically the one-electron and one-hole states.

Our model is based on several assumptions.

(1) We assume the excitonic state to be of a Wannier-Mott type. This assumption will be self-consistently verified: the calculated mean e-h distance in an exciton a_{ex} is large compared to the interatomic distance a_0 (about 12 and 3 Å, respectively). However, we have to ascertain that the Wannier-Mott condition $a_{ex} \gg a_0$ is on the verge of its validity. An alternative approach of Frenkel-type excitons to the PbI-based compounds was developed in Ref. 16. We believe, however, that the Wannier-Mott approach is more reasonable, because of considerable overlap of the electron orbitals in the perovskite layers, which hinders the electron and hole localization on one ion.

(2) We use the effective mass approximation (EMA) when solve the Schrödinger equation for the in-plane motion. This assumption is very crude, because the exciton radius is of the order of the in-plane period of the perovskite structure (about 6–7 Å). As a result, the role of nonparabolicity could be significant.

(3) We use macroscopic dispersionless susceptibilities for semiconductor and insulator layers, and get unphysical divergences in the one-particle potentials at the S/I interfaces. To avoid these divergences, we introduce transitional layers instead of abrupt interfaces. The width of this transitional layer Δ is an additional adjustable parameter of our model. Fortunately, the exciton binding energy does not depend significantly on this parameter.

(4) We use in our model the envelope-function approximation[17] (EFA) with the simplest boundary conditions (BC's) of a continuous wave function and probability current. Strictly speaking, such BC's become reasonable only if the Bloch (enveloped) functions of adjoining layers are similar. This is not the case of the S/I interfaces. However, it is well understood (see, e.g., Ref. 18) that if the carriers are mainly confined within well layers the EFA is not sensitive to the BC's.

The structure of the paper is as follows. In Sec. II the model of quasi-2D excitons is presented and the impact of the image potentials on the e-h interaction and QW localizing potential is analyzed. In Sec. III the results of our calculations of the excitonic parameters for lead iodide compounds are given, and the comparison with the experimental data of Refs. 2, 3, 5, 6, and 19 is discussed.

II. EXCITONS IN SEMICONDUCTOR/INSULATOR SUPERLATTICES: ROLE OF THE IMAGE POTENTIALS

Following the approach of Ref. 5, we treat the PbI-based self-organized structures as S/I SL's composed of alternating barriers and wells (insulator and semiconductor layers, respectively), with thicknesses (dielectric constants) l_b (ε_b) and l_w (ε_w).

Within the Wannier-Mott and effective mass approximations the excitonic Schrödinger equation takes the form

$$\left\{-\frac{\hbar^2}{2m_e}\Delta_e - \frac{\hbar^2}{2m_h}\Delta_h + U(z_e, z_h, |\boldsymbol{\rho}_e - \boldsymbol{\rho}_h|)\right\}\Psi(\boldsymbol{r}_e, \boldsymbol{r}_h) = E\Psi(\boldsymbol{r}_e, \boldsymbol{r}_h). \quad (1)$$

Here $\boldsymbol{r}_i = (\boldsymbol{\rho}_i, z_i)$, $i = e, h$, $\boldsymbol{\rho}$ is a 2D in-plane vector, $\Psi(\boldsymbol{r}_e, \boldsymbol{r}_h)$ is the e-h (excitonic) wave function, and the e-h potential energy can be written as (see the Appendix)

$$U(z_e, z_h, |\boldsymbol{\rho}_e - \boldsymbol{\rho}_h|) = U^e(z_e) + U^h(z_h) + V(z_e, z_h, |\boldsymbol{\rho}_e - \boldsymbol{\rho}_h|). \quad (2)$$

Here $U^{e,h}(z)$ are the one-electron and one-hole potentials, which take into account the S/I conduction and valence band offsets, and the self-image interaction

$$U^{e,h}(z) = \mathcal{E}^{c,v} + \frac{e}{2}\tilde{\varphi}(z), \quad (3)$$

$$\tilde{\varphi}(z) = \lim_{\rho\to 0}\left[\varphi(z, z, \rho) - \frac{e}{\varepsilon\rho}\right], \quad (4)$$

where $\mathcal{E}^{c,v}$, ε are $\mathcal{E}_w^{c,v}$, ε_w and $\mathcal{E}_b^{c,v}$, ε_b inside wells and barriers, respectively, and

$$V(z_e, z_h, |\boldsymbol{\rho}_e - \boldsymbol{\rho}_h|) = -e\,\varphi(z_e, z_h, |\boldsymbol{\rho}_e - \boldsymbol{\rho}_h|) \quad (5)$$

is the image-potential-mediated e-h interaction. Here the

function symmetrical over the electron and hole coordinates, $\varphi(z_e, z_h, |\boldsymbol{\rho}_e - \boldsymbol{\rho}_h|)$, is the electrostatic potential at point $\boldsymbol{r}_e = (\boldsymbol{\rho}_e, z_e)$ of a hole at point $\boldsymbol{r}_h = (\boldsymbol{\rho}_h, z_h)$. The exact expression for it as well as the proof of Eqs. (3)–(5) are in the Appendix [we regularize the electrostatic energy of the point charge, evaluating the limit in Eq. (4)].

In order to simplify the calculations, we assume that the excitonic wave function with the center of mass momentum $\boldsymbol{K} = \boldsymbol{0}$ takes the form

$$\Psi(\boldsymbol{r}_e, \boldsymbol{r}_h) = \psi^e(z_e)\psi^h(z_h)R_m(\rho)\exp(im\varphi), \tag{6}$$

i.e., the lowest order of perturbation theory over the ratio of the e-h interaction to the MQW localizing potential. Here the functions $\psi^{e,h}(z)$ are the solutions of the one-electron and one-hole Schrödinger equations for motion perpendicular to the SL planes and m and $R_m(\rho)$ are the exciton angular momentum and the in-plane wave function. Such an assumption can be justified by the fact that the band offsets in PbI-based compounds are much larger than the exciton binding energies (about 2 and 0.3 eV, respectively; see Sec. III).

Thus our calculation involves two successive steps: (A) we find the MQW one-electron and one-hole wave functions of perpendicular motion, and (B) we solve the Schrödinger equation for the in-plane excitonic wave function.

A. Self-image potential and one-particle QW-confined states in *S/I* superlattices

Let us consider the one-electron and one-hole Schrödinger equations for motion perpendicular to the SL planes:

$$\left[-\frac{\hbar^2}{2m_{e,h}}\frac{d^2}{dz^2} + U^{e,h}(z)\right]\psi^{e,h}(z) = E^{e,h}\psi^{e,h}(z), \tag{7}$$

where the one-electron and one-hole potentials $U^{e,h}$ depend on the coordinate perpendicular to the layers only and take the forms (see the Appendix)

$$U^{e,h}(z) = \mathcal{E}_w^{c,v} + \frac{e}{2}\int_0^\infty \frac{q\,dq}{2\pi}\left[\varphi(z,z,q) - \frac{2\pi e}{\varepsilon_w q}\right], \tag{8}$$

$$\varphi(z,z,q) = \frac{2\pi e}{\varepsilon_b q}\frac{1}{\sinh[q_0]}\Big\{2\alpha\beta\sinh[ql_b]\cosh[q(2z+l_w)] + \alpha^2\sinh[q(l_b+l_w)] + \beta^2\sinh[q(l_b-l_w)]\Big\}. \tag{9}$$

Here $-l_w < z < 0$ and q_0 is a solution of the secular Equation (A6). To obtain these formulas for $0 < z < l_b$, one should make in Eqs. (8) and (9) the substitutions $\varepsilon_w \leftrightarrow \varepsilon_b$, $l_b \leftrightarrow l_w$, and $z \leftrightarrow -z$.

Near the interfaces the self-image terms Eqs. (8) and (9) are the Coulomb-like interactions with the nearest image charge. For example, near the interface $z = 0$

$$U(z) \sim \frac{e^2}{4}\frac{\varepsilon_w - \varepsilon_b}{\varepsilon_w + \varepsilon_b}\frac{1}{z} \times \begin{cases} \varepsilon_w^{-1}, & z < 0, \\ \varepsilon_b^{-1}, & z > 0. \end{cases} \tag{10}$$

A charge in a semiconductor (insulator) layer is repulsed from (attracted towards) the interface. It is a well-known property of the image potentials. However, we cannot leave the divergent terms in Eq. (8), which are unphysical and appear in our model as a result of the unrealistic assumption of local dielectric susceptibility changing abruptly at the interfaces. (The approximation of constant dielectric susceptibility is valid only if the corrections to the electron and hole energies are small compared to E_g.) In order to avoid such Coulomb divergences we introduce transitional layers instead of abrupt interfaces, where the one-particle potential changes linearly between the boundary values determined by Eq. (8) (see Fig. 1, top). The transitional layer width Δ is an additional adjustable parameter of our model, of the order of the interatomic distance.

Large band offsets (and, as a consequence, barrier heights) allow us to neglect the tunneling between neighboring QW layers, and to use in Eq. (7) only the lowest-miniband wave functions of the form

$$\psi_{0,k}^{e,h}(z) = e^{ikz}u_0^{e,h}(z). \tag{11}$$

Here $u_0^{e,h}(z)$ and $E_0^{e,h}(z)$ are the ground state solutions of Eq. (7). Typical ground state solutions of Eq. (7) are shown in Fig. 1.

The self-image potential in Eq. (7) causes first of all an increase of the one-particle energies and thus a blueshift of the e-h band gap transitions. The physical reason for this is the repulsion of QW localized electrons and holes from the interfaces. However, the attraction of electrons and holes in the barrier to the interface manifests itself

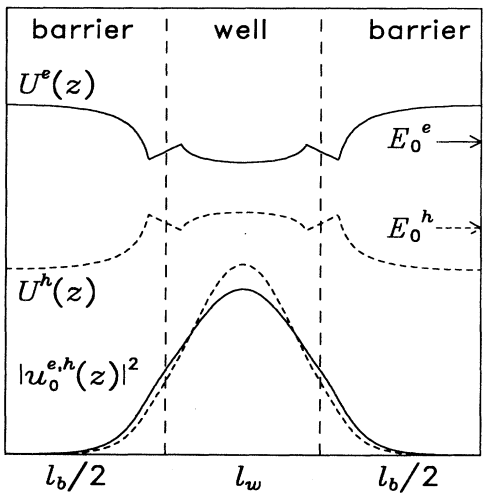

FIG. 1. One-electron (solid line) and one-hole (dashed line) potentials in a semiconductor/insulator superlattice (on the top) and corresponding ground state wave functions (on the bottom). The positions of the one-electron and one-hole ground state energies are shown by solid and dashed arrows.

in the appearance of additional potential minima near the interface, inside the barrier layers (see Fig. 1, top) and in wave function tails in the interface region (clearly seen in the bottom part of Fig. 1). As a result, there is a redshift of e-h band gap energies. Unfortunately, the calculated relative magnitude of these blue- and redshifts is very sensitive to the parameters of our model: the band offsets and the width of the transition layer. As a result, we cannot reliably predict the band gap energies within our model. [Experimentally, the exciton formation energy is almost constant, while the band gap opens up as n increases (see Fig. 8 in Ref. 3).] Our calculation of electron and hole eigenstates is thus no more than an intermediate step for evaluation of the exciton parameters. Fortunately, the latter are not very sensitive to the details of the one-electron and one-hole perpendicular wave functions.

However, on the grounds of the comparison to the experiment, we can at least exclude the case of small conduction or valence band offsets, when interface rather than QW localized states appear within our model. Such interface localization in PbI-based compounds may be excluded, because one of its consequences would be a splitting of the excitonic states, which is not observed experimentally. That is why we assume equal and large conduction and valence band offsets in our calculations.

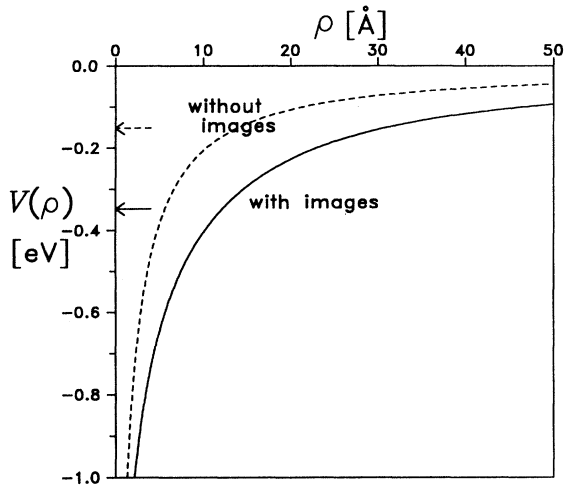

FIG. 2. Averaged image-potential-mediated electron-hole interaction in a S/I SL (solid line). Averaged electron-hole interaction without image corrections is also shown (dashed line). Corresponding positions of the exciton binding energies are shown by solid and dashed arrows.

B. Image-potential-mediated electron-hole interaction in S/I superlattices

The excitonic Schrödinger equation for the in-plane motion takes the form

$$-\frac{\hbar^2}{2\mu}\left(\frac{d^2}{d\rho^2}+\frac{1}{\rho}\frac{d}{d\rho}-\frac{m^2}{\rho^2}\right)R_m+V(\rho)R_m=ER_m, \quad (12)$$

where m is the exciton angular momentum, $\mu^{-1}=m_{\|e}^{-1}+m_{\|h}^{-1}$ is the reduced mass of the in-plane motion, and

$$V(\rho)=\int dz_e\int dz_h\,|u_0^e(z_e)|^2\,|u_0^h(z_h)|^2\,V(z_e,z_h,\rho) \quad (13)$$

is the averaged image-potential-mediated e-h interaction. Here

$$V(z_e,z_h,\rho)=-\frac{e}{2\pi}\int_0^\infty \varphi(z_e,z_h,q)J_0(q\rho)q\,dq, \quad (14)$$

where J_0 is the Bessel function, and the function φ is defined in the Appendix [see Eqs. (A4)–(A7)]. At large distances ρ (small q) $V(z_e,z_h,\rho)$ does not depend on the transverse coordinates $z_{e,h}$ and assumes a Coulomb-like dependence with some effective dielectric constant averaged over the SL,

$$V(z_e,z_h,\rho)=V(\rho)=-\frac{e^2}{\varepsilon^*\rho},$$

$$\varepsilon^*=\sqrt{\varepsilon_w\varepsilon_b\,\frac{\varepsilon_w l_w+\varepsilon_b l_b}{\varepsilon_b l_w+\varepsilon_w l_b}}. \quad (15)$$

At small ρ the potential $V(z_e,z_h,\rho)$ diverges logarithmically, like a 2D Coulomb potential.

The typical dependence of the averaged potential on ρ and the position of the exciton ground state are shown in Fig. 2 by a solid line and arrow. The averaged potential appears to be more localizing in comparison with that calculated without the image corrections (see dashed line and arrow in Fig. 2) due to the additional dipole-dipole interaction of an exciton with its images. This fact is the physical reason for the dielectric confinement of excitons in S/I SL's.

III. RESULTS AND DISCUSSION

Let us discuss first of all how we have chosen our model's adjustable parameters, i.e., conduction and valence band offsets $\mathcal{E}_{b,w}^{c,v}$, dielectric constants $\varepsilon_{b,w}$, perpendicular masses $m_{\perp e,h}$, reduced in-plane exciton mass μ, thicknesses of barrier and well layers $l_{b,w}$, and transition layer width Δ. Some of these parameters may be deduced from the known experimental data (see Table I); others are obtained by a fitting procedure.

(1) As was argued above, we have supposed equal conduction and valence band offsets, and taken

$$\mathcal{E}_w^{c,v}=0,\quad \mathcal{E}_b^{c,v}=\frac{E_g^b-E_g^w}{2} \quad (16)$$

for the C_n-PbI_4 family. Here $E_g^b=5.5$ eV and $E_g^w=1.68$ eV are the band gaps of $C_{12}H_{25}NH_2$ and C_1-PbI_3 materials, which are believed to have the same structure as insulator (barrier) and semiconductor (well) materials in the C_n-PbI_4 family. (For $n=12$ at least; we have

also assumed the same band offsets for all other n.) A different procedure (see below) was used to determine $\mathcal{E}^{c,v}_{b,w}$ for the PhE-Pb_mI_{3m+1} family, because we have not found in the literature the band gap of the corresponding organic material $C_6H_5C_2H_4NH_2$.

(2) The x-ray data on the geometric positions of iodine atoms allow us to deduce "nominal" thicknesses of barrier and well layers $l^0_{b,w}$ in all PbI compounds (see Table I). However, real thicknesses $l_{b,w}$ may differ from these values due to some effective ionic radius of the interface-located iodine atoms R_I,[3]

$$l_w = l^0_w + 2R_{\rm I}, \quad l_b = l^0_b - 2R_{\rm I}. \tag{17}$$

We assumed R_I to be the same for all PbI compounds and obtained its value (about 0.8 Å) from fitting our theory to the experimental data on C_{10}-PbI_4.

(3) We have assumed $\varepsilon_b = 2.1$ for the C_n-PbI_4 and 2.34 for the PhE-Pb_mI_{3m+1} family, i.e., the values in the corresponding parent organic materials (see Table I). In order to deduce ε_w, we have used the experimental data (see Table I) on the high-frequency dielectric constant ε_∞ of lead iodide compounds,

$$\varepsilon_\infty = \frac{\varepsilon_w l_w + \varepsilon_b l_b}{l_w + l_b}, \tag{18}$$

and Eqs. (17). Thus we have guaranteed the correct experimental value of the high-frequency dielectric constant ε_∞.

(4) We have obtained the values of perpendicular masses and the transition layer width (assumed to be the same for all compounds) by means of fitting the calculated band gap energy of C_{10}-PbI_4 to the experimental data (Table I). As was mentioned above, this procedure is very sensitive to these adjustable parameters. Fortunately, the exciton parameters are not too sensitive to these parameters [the electron and hole perpendicular wave functions are needed only for averaging the e-h interaction, Eq. (13)]. We have postulated the same values of perpendicular masses and transition layer width for the PhE-Pb_mI_{3m+1} family and estimated its $E^b_g = 4.5$ eV

TABLE I. Experimental and calculated parameters of lead iodide compounds: high-frequency dielectric constant ε_∞, band gap E_g, geometric semiconductor and insulator layer thicknesses l^0_w and l^0_b, exciton binding energies $E_{\rm ex}$, diamagnetic factors c_0, and mean radii $a_{\rm ex}$.

Compound	ε_∞	E_g (eV) (T=1.6 K)	l^0_w (Å)	l^0_b (Å)	$E_{\rm ex}$ (meV) expt.	$E_{\rm ex}$ (meV) theor.	c_0 $\left(10^{-7}\frac{\rm eV}{\rm T^2}\right)$ expt.	c_0 $\left(10^{-7}\frac{\rm eV}{\rm T^2}\right)$ theor.	$a_{\rm ex}$ (Å) theor.
C_nH_{2n+1}-NH_2	2.1[a] 2.07[c] (n=10)	5.5[b] (n=12)							
C_6H_5-$C_2H_4NH_2$	2.34[c]	4.5[d]							
C_1-PbI_3	6.5[g]	1.678[e]			45[e] 37[g]	63[f]	27[e]	14.2[f]	33.0[f] 28[g]
C_4-PbI_4		2.88[b]	6.36[h]	8.53[b] 8.81[i]	290 ± 20[b]	287[f]		2.25[f]	13.2[f]
C_6-PbI_4		2.88[b]	6.36[h]	10.03[i]		299[f]	2.16–3.53[k]	2.21[j]	13.1[f]
C_8-PbI_4		2.88[b]	6.36[h]	12.02[i]		310[f]		2.19[f]	13.0[f]
C_9-PbI_4		2.88[b]	6.36[h]	13.53[i]	320 ± 30[e]	315[f]		2.19[f]	13.0[f]
C_{10}-PbI_4	3.24[l]	2.88[b] 2.87[k]	6.36[h]	14.89[i]	320 ± 30[e]	321[j]	1.7[l] 0.7 ± 0.4[m]	2.18[f]	13.0[f]
C_{12}-PbI_4	3.39[h]		6.36[h]	18.15[h]	310 ± 30[b]	330[f]		2.17[f]	13.0[f]
PhE-PbI_4	4.41[h]	2.58[h] 2.57[k]	6.36[h] 6.41[n]	9.82[h] 9.85[n]	220 ± 30[h]	250[f]		2.60[f]	14.2[f]
PhE-Pb_2I_7		2.34[h] 2.32[k]	12.70[h] 13.05[n]	9.71[n]	170 ± 30[h]	190[f]		3.50[f]	16.5[f]

[a] *CRC Handbook of Chemistry and Physics*, 63rd ed., edited by R. C. West (Chemical Rubber Company, Boca Raton, FL, 1983).
[b] Reference 3.
[c] T. Ishihara, X. Hong, J. Ding, and A. V. Nurmikko, Surf. Sci. **267**, 323 (1992).
[d] Estimated value (see the text).
[e] Reference 6.
[f] Theory, this work.
[g] M. Hirasawa, T. Ishihara, T. Goto, K. Uchida, and N. Miura, Physica B **201**, 427 (1994).
[h] Reference 5.
[i] J. Takahashi (unpublished).
[j] Fitted number, this work.
[k] Reference 16.
[l] Reference 19.
[m] M. Hirasawa, T. Ishihara, T. Goto, K, Uchida, and N. Miura, Solid State Commun. **86**, 479 (1993).
[n] Reference 4.

from the inverse fitting procedure.

(5) The most significant parameter is the reduced in-plane exciton mass μ. Examples of calculated E_{ex} and a_{ex} dependences in C_{10}-PbI_4 on μ are shown in Fig. 3. We assumed μ to be the same for all PbI compounds and obtained its value ($0.17m_0$) from fitting our theory to the experimental data on the exciton binding energy E_{ex} and the diamagnetic factor $c_0 = e^2a_{ex}^2/8\mu$. E_{ex} was fitted to the experimental value for C_{10}-PbI_4, and c_0 to that for C_6-PbI_4, due to a large range of the experimental values for C_{10}-PbI_4 (see Table I). The second parameter obtained within this fitting procedure is the effective ionic radius R_I (see above).

It is noteworthy that our fitted reduced mass is twice as large as that obtained previously.[3,5] This larger value looks more trustworthy for such wide band gap materials as lead iodide compounds. The basic reason for obtaining a larger value of μ is our taking into account the self-image terms, which was not done previously. In Refs. 3 and 5 an infinite-barrier model was used for the perpendicular wave functions, $\psi^{e,h} \propto \sin(2\pi z/l_w)$. As a result of these more QW-confined wave functions (as compared to our wave functions with tails into the barrier layers, Fig. 1) the averaged e-h interaction $V(\rho)$ becomes more confined too, and one needs a smaller μ to fit the same experimental value of E_{ex}.

As a result, we have got for C_n-PbI_4 $\mu = 0.17m_0$, $R_I = 0.8$Å, $m_{\perp e} = 0.2m_0$, $m_{\perp h} = 0.5m_0$, $m^b_{\perp e,h} = 2.5m_0$, $\varepsilon_b = 2.1$, $\varepsilon_w = 6.05$, $\Delta = 2$ Å, $E_g^w = 1.68$ eV, and $E_g^b = 5.5$ eV. For PhE-Pb_mI_{3m+1} $\varepsilon_b = 2.34$, $\varepsilon_w = 6.48$, and $E_g^b = 4.5$ eV; the other parameters are the same.

Let us discuss now the results of our calculations of E_{ex}, c_0, and a_{ex}, which are shown in Table I and in Figs. 3 and 4. One can see that, although our fitting procedure was rather crude and the number of unknown material parameters was large, the theoretical results show reasonable agreement with the experimental data for the whole lead iodide family.

The fact that our theory gives different excitonic parameters for different members of the C_n-PbI_4 family clearly demonstrates the role of the SL effects. With an increase of n the ratio l_b/l_w increases. Experimentally there are some hints that E_{ex} increases too (see the experimental points in Fig. 4 and Table I). The calculated dependence of E_{ex} on l_b/l_w (shown in Fig. 4 by a solid line) clearly demonstrates this tendency. The calculated dependence saturates very soon at a value which corresponds to the exciton binding energy in a single quantum well embedded into the corresponding organic material.

The comparison of calculated binding energies for C_6-PbI_4 and PhE-PbI_4 (300 and 250 meV, respectively), which have the same barrier and well thicknesses but different dielectric constant ratios ($\varepsilon_w/\varepsilon_b = 2.88$ for C_6-PbI_4 and $\varepsilon_w/\varepsilon_b = 2.77$ for PhE-PbI_4), clearly demonstrates that, due to the dielectric confinement, the exciton binding energy increases with increase of the differ-

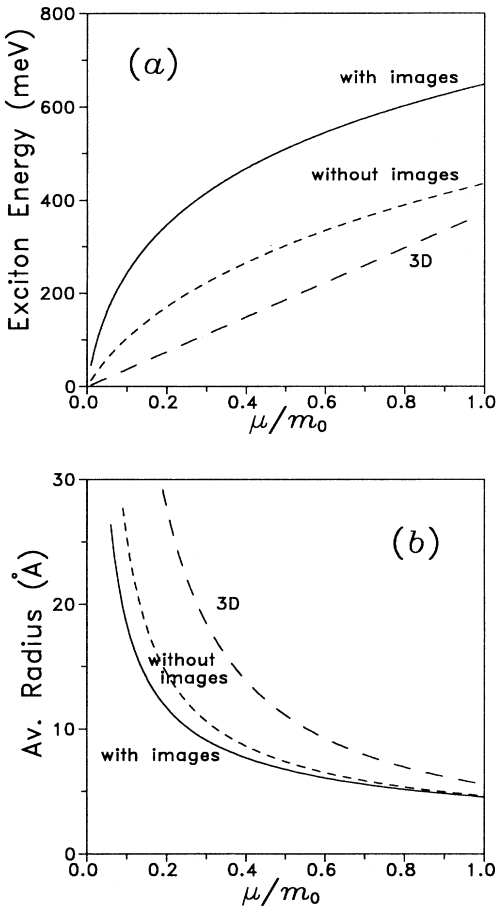

FIG. 3. Exciton binding energy (a) and averaged radius (b) as functions of reduced exciton mass in C_{10}-PbI_4 with allowance for image and QW localizing potentials (solid lines), only QW potential (short dashes), and in a homogeneous 3D semiconductor, made of the well material (long dashes).

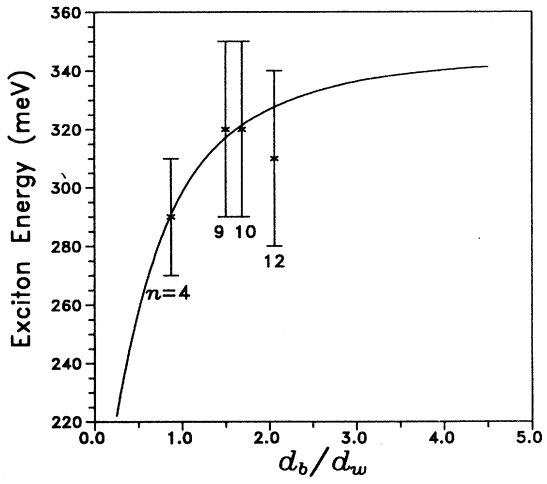

FIG. 4. Exciton binding energy as a function of layer thickness ratio. The experimental data on corresponding C_n-PbI_4 compounds are shown by asterisk and bars.

ence between the semiconductor and insulator dielectric constants. In the case of the double well layer in PhE-Pb_2I_7 the average distances between carriers and their images are larger and image potentials are weaker than in PhE-PbI_4, and the exciton appears to be less bound.

The net magnitude of the dielectric confinement effect can be seen also from Fig. 3, where the exciton parameters as functions of the reduced mass are shown as calculated with and without image charge effects (solid and short dashed lines, respectively). For comparison, we show also the same dependences calculated for a homogeneous 3D semiconductor without barrier layers at all (long dashes). For example, we get (for $\mu = 0.17m_0$) $E_{ex} = 320$ meV for both dielectric and quantum well confinement, 152 meV for quantum well confinement only (i.e., calculated with $\varepsilon_b = \varepsilon_w$ and the other parameters the same), and 63 meV without any confinement at all. The last number is of the order of the experimental value of E_{ex} in C_1-PbI_3 (45 meV, see Table I). We see that in this case the quasi-2D QW confinement enhances the exciton binding energy by 2.4 times only (i.e., less than 4, the limiting value for 2D confinement), and as much as 5 times when the image charges are taken into account.

To conclude, we have developed a theoretical model for calculation of the exciton binding energies in semiconductor/insulator superlattices with special emphasis on the lead iodide based self-organized compounds. This approach takes into account the image potentials and demonstrates good agreement with the experimental data. Thus we believe that the dielectric confinement model explains the exciton enhancement in lead iodide compounds, and our theory offers a good starting point for further discussion of their excitonic properties.

ACKNOWLEDGMENTS

The authors are thankful to Professor L. V. Keldysh and to Professor R. A. Suris for helpful discussions. The work was supported in part by the Russian Ministry of Science Program "Nanostructures," Research Grant No. 1-041.

APPENDIX: ELECTROSTATIC ENERGY OF AN EXCITON IN A S/I SUPERLATTICE

Let us calculate first of all, following Guseinov,[14] the electrostatic potential $\varphi(z, z_0, |\boldsymbol{\rho}_e - \boldsymbol{\rho}_h|)$ of a charge e, located at point $\boldsymbol{r}_0 = (\boldsymbol{\rho}_0, z_0)$ in a semiconductor layer of a S/I SL. It is the solution of Poisson's equation

$$\Delta\varphi = -\frac{4\pi e}{\varepsilon}\delta(\boldsymbol{r} - \boldsymbol{r}_0) \tag{A1}$$

with the boundary conditions

$$\varphi_b = \varphi_w, \quad \varepsilon_b\frac{\partial\varphi_b}{\partial z} = \varepsilon_w\frac{\partial\varphi_w}{\partial z}. \tag{A2}$$

Here $\varepsilon = \varepsilon_w$ inside the well (e.g., for $-l_w < z_0 < 0$) and ε_b ($0 < z_0 < l_b$). The solution takes the form

$$\varphi(z, z_0, |\boldsymbol{\rho} - \boldsymbol{\rho}_0|) = \int \frac{d^2q}{(2\pi)^2}\exp\{\boldsymbol{q}\cdot(\boldsymbol{\rho} - \boldsymbol{\rho}_0)\}\varphi(z, z_0, q), \tag{A3}$$

where $q = |\boldsymbol{q}|$, $\boldsymbol{q}$ is the in-plane wave vector, and the Fourier-transformed potential is

$$\varphi(z, z_0, q) = \frac{2\pi e}{\varepsilon q}e^{-q|z-z_0|} + C_+e^{qz} + C_-e^{-qz}, \tag{A4}$$

where (for $-l_w < z, z_0 < 0$)

$$C_+ = \frac{2\pi e}{\varepsilon_w q}\,\frac{\exp[q(z_0 + l_w)]\zeta\sinh[ql_b] + \exp[-qz_0](D - \lambda\eta)}{2\eta\sinh[q_0]},$$

$$C_- = \frac{2\pi e}{\varepsilon_w q}\,\frac{\exp[-q(z_0 + l_w)]\zeta\sinh[ql_b] + \exp[qz_0](D - \lambda\eta)}{2\eta\sinh[q_0]}. \tag{A5}$$

$\lambda = \exp[q_0]$ and q_0 is a positive solution of the SL secular equation

$$\begin{aligned}
&\eta\cosh[q_0] = \alpha^2\cosh[q(l_b + l_w)] - \beta^2\cosh[q(l_b - l_w)],\\
&D = \alpha^2\exp[q(l_b + l_w)] - \beta^2\exp[-q(l_b - l_w)],\\
&\eta = \varepsilon_b/\varepsilon_w, \quad \alpha = (1 + \eta)/2, \quad \beta = (1 - \eta)/2, \quad \zeta = 2\alpha\beta.
\end{aligned} \tag{A6}$$

Thus,

$$\begin{aligned}
\varphi(z, z_0, q) = -\frac{2\pi e}{\varepsilon_w q}\sinh(q|z - z_0|) + \frac{2\pi e}{\varepsilon_b q\sinh[q_0]}\Big\{&2\alpha\beta\sinh[ql_b]\cosh[q(z + z_0 + l_w)]\\
&+\{\alpha^2\sinh[q(l_b + l_w)] + \beta^2\sinh[q(l_b - l_w)]\}\cosh[q(z - z_0)]\Big\}.
\end{aligned} \tag{A7}$$

To obtain the corresponding formula for $0 < z, z_0 < l_b$, one should make in Eq. (A7) the substitutions $\varepsilon_w \leftrightarrow \varepsilon_b$, $l_b \leftrightarrow l_w$, $z \leftrightarrow -z$, and $z_0 \leftrightarrow -z_0$. When z and z_0 belong to different layers the potential $\varphi(z, z_0, q)$ does not contain a

singular part.

When the charge and observation point are in neighboring layers the potential is

$$\varphi(z,z_0,q)=\frac{2\pi e}{\varepsilon_b q\sinh[q_0]}\Big\{\alpha\sinh[q(l_b+l_w)]\cosh[q(z-z_0)]+\beta\sinh[q(l_b-l_w)]\cosh[q(z+z_0)]$$
$$+\beta\{2\alpha^2\sinh[ql_b]\sinh[ql_w]-\sinh[q_0]\}\sinh[q(z+z_0)]+\alpha\{2\beta^2\sinh[ql_b]\sinh[ql_w]-\sinh[q_0]\}\sinh(q|z-z_0|)\Big\}. \tag{A8}$$

Equations (A4)–(A8) are simplified Guseinov formulas (see Ref. 14).

Using Eqs. (A3)–(A8), we can write the electrostatic potential of an exciton ($\boldsymbol{r}_e$ and $\boldsymbol{r}_h$ being the electron and the hole coordinates) as

$$\Phi(\mathbf{r},\boldsymbol{r}_e,\boldsymbol{r}_h)=\varphi(z,z_h,|\boldsymbol{\rho}-\boldsymbol{\rho}_h|)-\varphi(z,z_e,|\boldsymbol{\rho}-\boldsymbol{\rho}_e|). \tag{A9}$$

Let us calculate now the full electrostatic energy of an exciton in a S/I SL

$$W(z_e,z_h,|\boldsymbol{\rho}_e-\boldsymbol{\rho}_h|)=\frac{1}{8\pi}\int_{V_{\rm SL}}\boldsymbol{E}\cdot\boldsymbol{D}\,d^3r, \tag{A10}$$

where $V_{\rm SL}$ is the SL volume. The integral in Eq. (A10) can be split into a sum of integrals over well and barrier layers $V_{w,n}$ and $V_{b,n}$ with corresponding dielectric constants ε_w and ε_b ($n=0,\pm1,\pm2,\ldots$; $n=0$ corresponds to the well to which the exciton is confined). Using subsequently Green's formula, the electrostatic boundary conditions Eq. (A2), the Poisson equation Eq. (A1), and Eq. (A9), we get

$$\begin{aligned}W&=\frac{1}{8\pi}\sum_n\left[\varepsilon_w\int_{V_{w,n}}d^3r+\varepsilon_b\int_{V_{b,n}}d^3r\right][\nabla\Phi\cdot\nabla\Phi]\\&=\frac{e}{2}\left[\Phi(\boldsymbol{r}_h,\boldsymbol{r}_e,\boldsymbol{r}_h)-\Phi(\boldsymbol{r}_e,\boldsymbol{r}_e,\boldsymbol{r}_h)\right]\\&=\frac{e}{2}\left[\tilde\varphi(z_e)+\tilde\varphi(z_h)-\varphi(z_e,z_h,|\boldsymbol{\rho}_e-\boldsymbol{\rho}_h|)-\varphi(z_h,z_e,|\boldsymbol{\rho}_e-\boldsymbol{\rho}_h|)\right],\end{aligned} \tag{A11}$$

where

$$\begin{aligned}\tilde\varphi(z)&=\lim_{\rho\to0}\left[\varphi(z,z,\rho)-\frac{e}{\varepsilon\rho}\right]\\&=\int_0^\infty\frac{q\,dq}{2\pi}\left[\varphi(z,z,q)-\frac{2\pi e}{\varepsilon q}\right].\end{aligned} \tag{A12}$$

It is well known that the electrostatic energy Eq. (A10) contains divergent terms, which correspond to infinite self-energies of point charges. These terms do not depend on the electron and hole positions and do not contribute to their equations of motion. They can be extracted from Eq. (A10), and such a renormalizing procedure is implicit in Eqs. (A11) and (A12).

Finally, we get the following expression for the regularized electrostatic energy of the exciton:

$$W(z_e,z_h,|\boldsymbol{\rho}_e-\boldsymbol{\rho}_h|)$$
$$=\frac{e}{2}\left[\tilde\varphi(z_e)+\tilde\varphi(z_h)-2\varphi(z_e,z_h,|\boldsymbol{\rho}_e-\boldsymbol{\rho}_h|)\right]. \tag{A13}$$

In order to obtain the excitonic Hamiltonian, we have to add Eq. (A13) to the usual kinetic and MQW localizing energies.

* Electronic address: tikh@gpi.ru
† Electronic address: terry@ue.ipc.hiroshima-u.ac.jp

[1] S. S. Nagapetyan, Yu. I. Dolzhenko, E. R. Arakelova, V. Koshkin, Yu. T. Struchkov, and V. E. Shklover, Zh. Neorg. Khim. **33**, 2806 (1988) [Russ. J. Inorg. Chem. **33**, 1614 (1988)].
[2] T. Ishihara, J. Takahashi, and T. Goto, Solid State Commun. **69**, 933 (1989).
[3] T. Ishihara, J. Takahashi, and T. Goto, Phys. Rev. B **42**, 11 099 (1990).
[4] J. Calabrese, N. L. Jones, R. L. Harlow, N. Herron, D. L. Thorn, and Y. Wang, J. Am. Chem. Soc. **113**, 2328 (1991).
[5] X. Hong, T. Ishihara, and A. V. Nurmikko, Phys. Rev. B **45**, 6961 (1992).
[6] T. Ishihara, J. Lumin. **60&61**, 269 (1994).
[7] M. Era, S. Morimoto, T. Tsutsui, and S. Saito, Appl. Phys. Lett. **65**, 676 (1994).
[8] N. S. Rytova, Vestn. Mosk. Univ. **3**, 30 (1967).
[9] L. V. Keldysh, Pis'ma Zh. Eksp. Teor. Fiz. **29**, 716 (1979) [JETP Lett. **29**, 658 (1979)].

[10] E. Hanamura, N. Nagaosa, M. Kumagai, and T. Takagahara, Mater. Sci. Eng. **B1**, 255 (1988).
[11] T. Takagahara, Phys. Rev. B **47**, 4569 (1993).
[12] D. B. Tran Thoai, R. Zimmermann, M. Grundmann, and D. Bimberg, Phys. Rev. B **42**, 5906 (1990).
[13] J. Cen and K. K. Bajaj, in *Proceedings of the 22nd ICPS, Vancouver, 1994*, edited by M. L. W. Thewalt (World Scientific, Singapore, in press).
[14] R. R. Guseinov, Phys. Status Solidi B **125**, 237 (1984).
[15] L. Wendler and B. Hartwig, J. Phys. Condens. Matter **3**, 9907 (1991).
[16] T. Kataoka, T. Kondo, R. Ito, S. Sasaki, K. Uchida, and S. Miura, Phys. Rev. B **47**, 2010 (1993).
[17] G. Bastard, *Wave Mechanics Applied to Semiconductor Heterostructures* (Les Editions de Physique, Les Ulis, France, 1988).
[18] S. G. Tikhodeev, Solid State Commun. **78**, 339 (1991).
[19] C. Xu, H. Sakakura, T. Kondo, S. Takeyama, N. Miura, Y. Takahashi, K. Kumata, and R. Ito, Solid State Commun. **79**, 249 (1991).